

RESEARCH

Open Access



Prevention of severe lung immunopathology associated with influenza infection through adeno-associated virus vector administration

Eun Ah Choi¹, Hi Jung Park¹, Sung Min Choi¹, Jae Il Lee^{2,5*}  and Kyeong Cheon Jung^{2,3,4*}

Abstract

Background Influenza A viruses (IAVs) have long posed a threat to humans, occasionally causing significant morbidity and mortality. The initial immune response is triggered by infected epithelial cells, alveolar macrophages and dendritic cells. However, an exaggerated innate immune response can result in severe lung injury and even host mortality. One notable pathology observed in hosts succumbing to severe influenza is the excessive influx of neutrophils and monocytes into the lung. In this study, we investigated a strategy for controlling lung immunopathology following severe influenza infection.

Results To evaluate the impact of innate immunity on influenza-associated lung injury, we employed CB17.SCID and NOD.SCID mice. NOD.SCID mice exhibited slower weight loss and longer survival than CB17.SCID mice following influenza infection. Lung inflammation was reduced in NOD.SCID mice compared to CB17.SCID mice. Bulk RNA sequencing analysis of lung tissue showed significant downregulation of 827 genes, and differentially expressed gene analysis indicated that the cytokine-cytokine receptor interaction pathway was predominantly downregulated in NOD.SCID mice. Interestingly, the expression of the *Cxcl14* gene was higher in the lungs of influenza-infected NOD.SCID mice than in CB17.SCID mice. Therefore, we induced overexpression of the *Cxcl14* gene in the lung using the adeno-associated virus 9 (AAV9)-vector system for target gene delivery. However, when we administered the AAV9 vector carrying the *Cxcl14* gene or a control AAV9 vector to BALB/c mice from both groups, the morbidity and mortality rates remained similar. Both groups exhibited lower morbidity and mortality than the naive group that did not receive the AAV9 vector prior to IAV infection, suggesting that the pre-administration of the AAV9 vector conferred protection against lethal influenza infection, irrespective of *Cxcl14* overexpression. Furthermore, we found that pre-inoculation of BALB/c mice with AAV9 attenuated the infiltration of trans-macrophages, neutrophils and monocytes in the lungs following IAV infection. Although there was no difference in lung viral titers between the naive group and the AAV9 pre-inoculated group, pre-inoculation with AAV9 conferred lung injury protection against lethal influenza infection in mice.

*Correspondence:

Jae Il Lee

jaeil@snu.ac.kr

Kyeong Cheon Jung

jungkc66@snu.ac.kr

Full list of author information is available at the end of the article



© The Author(s) 2023. **Open Access** This article is licensed under a Creative Commons Attribution 4.0 International License, which permits use, sharing, adaptation, distribution and reproduction in any medium or format, as long as you give appropriate credit to the original author(s) and the source, provide a link to the Creative Commons licence, and indicate if changes were made. The images or other third party material in this article are included in the article's Creative Commons licence, unless indicated otherwise in a credit line to the material. If material is not included in the article's Creative Commons licence and your intended use is not permitted by statutory regulation or exceeds the permitted use, you will need to obtain permission directly from the copyright holder. To view a copy of this licence, visit <http://creativecommons.org/licenses/by/4.0/>. The Creative Commons Public Domain Dedication waiver (<http://creativecommons.org/publicdomain/zero/1.0/>) applies to the data made available in this article, unless otherwise stated in a credit line to the data.

Conclusions Our study demonstrated that pre-inoculation with AAV9 prior to IAV infection protected mouse lungs from immunopathology by reducing the recruitment of inflammatory cells.

Keywords Influenza A virus, Adeno-associated virus, Lung injury, Immunopathology, Inflammatory cells

Background

Influenza A viruses (IAVs) are enveloped single-stranded RNA viruses with eight segmented genes and are characterized by hemagglutinin (HA) and neuraminidase (NA) surface glycoproteins, which are the primary targets of neutralizing antibodies [1, 2]. These viruses exhibit rapid evolution with point mutations in viral proteins, known as ‘antigenic drift’, that allow them to evade immunity conferred by previous infection or vaccination and cause annual outbreaks [2, 3]. Severe morbidity and mortality associated with pandemic IAVs primarily result from lung injury caused by severe immunopathology and secondary bacterial infection [4]. The major observed pathology in the lungs of hosts with severe influenza is the massive influx of neutrophils and monocytes [5]. The initial immune response to IAV infection is the secretion of interferons by infected epithelial cells, alveolar macrophages and dendritic cells, followed by the recruitment of inflammatory cells such as neutrophils, monocytes/macrophages and natural killer cells, and finally the activation of adaptive immune cells, which contribute to virus clearance and host recovery [6].

Neutrophils can play both beneficial and detrimental roles during influenza infection [7]. Studies have shown that depleting neutrophils prior to sublethal IAV infection in mice, results in uncontrolled viral growth and increased mortality, indicating a protective role for neutrophils. These findings were further supported by subsequent studies [7–9], which highlighted the production of the antimicrobial peptide mCRAMP by neutrophils and their ability to induce the release of IL-1 β in alveolar macrophages [8]. Neutrophils also play a crucial role in directing the migration of influenza-specific CD8 T cells to the site of infection and maintaining CD8 T cell effector responses [9, 10]. However, another study demonstrated that a transcriptional signature of neutrophil accumulation in the lung during influenza infection could predict a lethal outcome [11]. In other words, attenuating rather than completely depleting neutrophils reduced mortality in mice, suggesting the need to dampen exaggerated neutrophilic inflammation to protect hosts from lethal influenza infection [11]. Upon exposure to IAVs, alveolar macrophages promote the recruitment of CCR2⁺Ly6C^{hi} inflammatory monocytes [6, 12]. These monocytes further differentiate into inflammatory monocyte-derived macrophages and inflammatory dendritic cells, which promote the recruitment of protective NK

cells [6, 12]. However, prolonged recruitment of inflammatory monocytes has been reported to contribute to the lethality of severe influenza infection, and depleting these cells has been shown to attenuate lung injury [13, 14].

Adeno-associated virus (AAV) is a nonenveloped single-stranded DNA parvovirus with a genome size of approximately 4.8 kb. Due to its nonpathogenic nature, low immunogenicity and broad tropism, AAV has emerged as a valuable tool for delivering therapeutic genes with long-term expression in both animals and humans [15, 16]. Following successful trials in hemophilia patients over a decade ago [17], AAV vectors have been extensively studied in clinical trials targeting various genetic diseases. The AAV genome consists of replication (rep) and capsid (cap) genes, with the genomic DNA flanked by two inverted terminal repeats (ITRs) [17, 18]. AAV vectors are constructed by replacing most of the viral genome with expression cassettes consisting of a promoter, a gene of interest and a poly A tail [19]. Once integrated into host cells, 3′-ITR serves as a primer for host DNA polymerase, generating a self-complementary intermediate comprising both plus and minus DNA strands [17, 18]. Interestingly, a previous study suggested that both plus and minus strand RNAs could be copied from the self-complementary intermediate DNA within the cytoplasm of AAV-transduced cells, due to the inherent promoter activity of 5′- and 3′-ITRs [20]. This process results in the formation of double-stranded RNA (dsRNA), triggering the cytoplasmic dsRNA sensor MDA5 in host cells. Sensing dsRNA leads to the production of IFN- β , which subsequently suppresses transgene expression [20]. However, it remains undetermined whether in vivo gene transduction using AAV vectors can also influence other immune responses, such as the response to IAV infection.

In this study, we employed CB17.SCID and NOD.SCID mice to investigate a strategy for controlling lung immunopathology following severe influenza infection. Our findings revealed that NOD.SCID mice exhibited reduced morbidity and mortality compared to CB17.SCID mice, which was associated with attenuated infiltration of neutrophils and inflammatory monocytes. Notably, *Cxcl14* gene expression was higher in the infected lungs of NOD.SCID mice than that of CB17.SCID mice, in contrast to other inflammatory cytokines and chemokines. Based on these findings, we attempted to overexpress the *Cxcl14* gene in the lungs of mice using

the AAV9 vector. Interestingly, mice receiving the AAV9 vector itself, independent of *Cxcl14* gene overexpression, exhibited significantly reduced mortality after IAV challenge compared to mice not receiving the AAV9 vector. Further analysis revealed that the increased survival was associated with decreased infiltration of neutrophils and trans-macrophages in the infected lungs. These results demonstrated the immunoregulatory potential of AAV9 vectors.

Results

Attenuated lung inflammation in NOD.SCID mice compared to CB17.SCID mice

To evaluate the impact of innate and adaptive immunity on influenza-associated lung injury, we utilized BALB/c,

CB17.SCID and NOD.SCID mice in our study. All three groups of mice were intranasally infected with a sublethal dose of IAV, and changes in body weight and mortality were monitored. Following influenza challenge, body weight progressively decreased in all mouse groups, with no difference in weight loss observed between BALB/c and CB17.SCID mice during the first six days (Fig. 1A). Then, BALB/c mice regained body weight and ultimately survived, while CB17.SCID mice failed to recover, resulting in 100% mortality as expected (Fig. 1B). In contrast, NOD.SCID mice exhibited slower weight loss and significantly prolonged survival compared to CB17.SCID mice (Fig. 1A, B).

These findings raised two possibilities: reduced viral replication or attenuated lung inflammation in NOD.

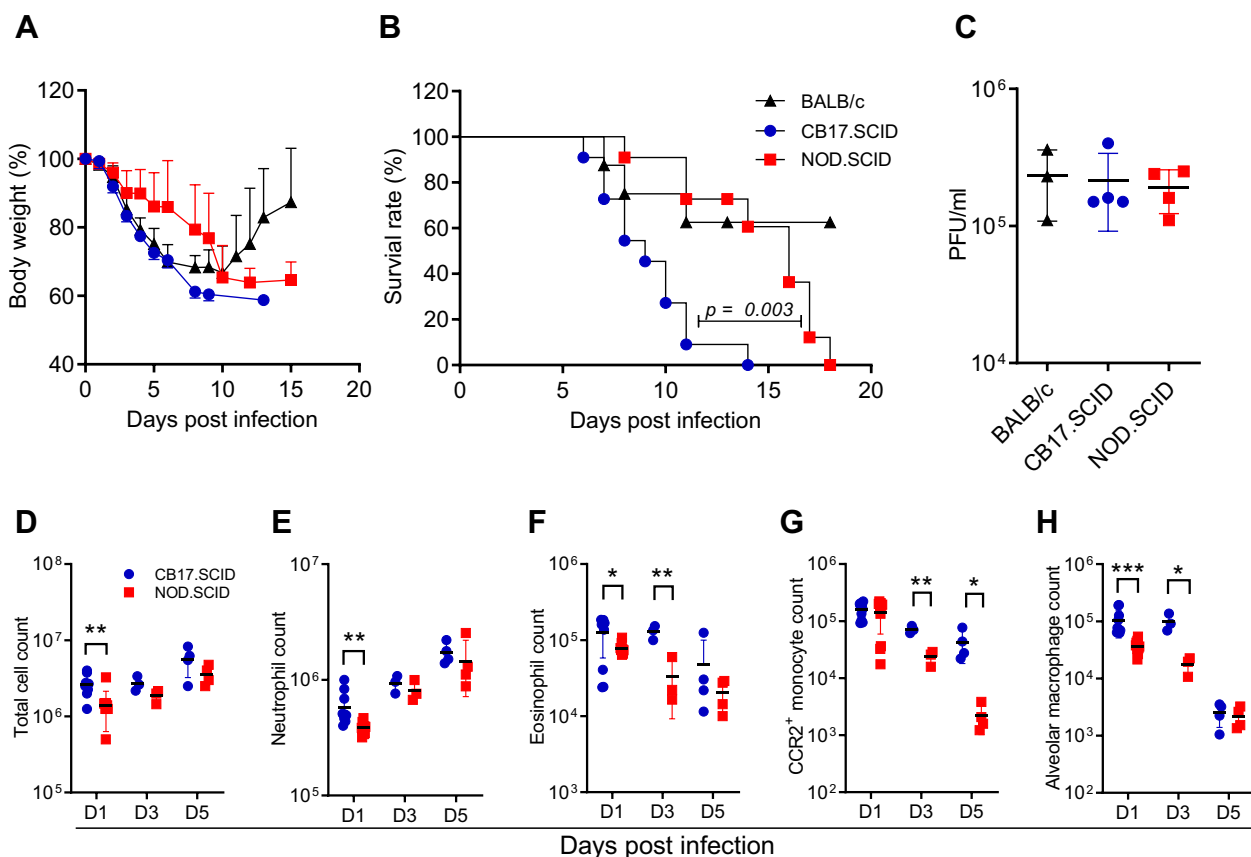


Fig. 1 Improved prognosis in NOD.SCID mice than CB17.SCID mice after IAV infection. **(A)** Body weight and **(B)** mortality were monitored in BALB/c, CB17.SCID, and NOD.SCID mice after infection with IAV. Cumulative data from three independent experiments ($n = 15$ per group) show attenuated weight loss and prolonged survival in NOD.SCID mice compared to the CB17.SCID control. Survival rate differences were statistically significant as determined by the log-rank (Mantel-Cox) test. **(C)** On day 5 post-infection, lungs were harvested from IAV-infected mice, and the virus titer was measured by plaque assay. Cumulative data from three mouse groups ($n = 5$ per group) show no difference in virus titers between the groups. **(D–G)** Immune cells were extracted from the lungs of CB17.SCID and NOD.SCID mice on days 1, 3, and 5 post-infection, with the absolute number of each immune cell type determined through flow cytometric analysis. Comparative evaluation of total cell counts **(D)**, neutrophils **(E)**, eosinophils **(F)**, CCR2⁺ inflammatory monocytes **(G)**, and alveolar macrophages **(H)** between the two groups was carried out. Cumulative data from two groups of mice ($n = 5$ per group) show statistically significant differences in immune cell counts, analyzed using an unpaired t-test. Statistical significance is indicated as follows: * $p < 0.05$; ** $p < 0.04$; *** $p < 0.001$

SCID mice compared to the other groups. To assess the first possibility, virus titers were measured using a plaque assay on homogenized lung tissue on day 5 post-infection. As shown in Fig. 1C, no difference was observed in viral titers among the three mouse groups. Subsequently, we evaluated the inflammatory response in infected lungs on day 1, day 3, and day 5 post-infection through flow cytometric analysis, which revealed attenuated infiltration of inflammatory cells in NOD.SCID lungs compared to CB17.SCID lungs (Fig. 1D). Notably, distinct kinetics were observed for granulocytes and inflammatory monocytes. The number of neutrophils and eosinophils was significantly lower in NOD.SCID mice than in CB17.SCID controls on day 1 and day 3 post-infection, and the difference between the two groups gradually diminished during the course of lung inflammation (Fig. 1E, F). Conversely, CCR2⁺ inflammatory monocytes, which are closely associated with the severity of inflammation in IAV infection [13], initially infiltrated the lungs of both groups in comparable quantities. However, the number of infiltrating cells declined more rapidly in NOD.SCID lung compared to the CB17.SCID control (Fig. 1G). These results are consistent with previous reports that inflammatory monocytes and neutrophils contribute to lethal lung injury in influenza and SARS-CoV infections [13, 21]. Additionally, studies have shown that CCR2 blockade reduces lung pathology associated with influenza infection and partially suppresses the neutrophil response in mice exposed to lethal IAV strains [11, 22]. Taken together, the attenuated infiltration of inflammatory monocytes and neutrophils in NOD.SCID mice may contribute to their prolonged survival.

In contrast to granulocytes and inflammatory monocytes, alveolar macrophages, which are long-lived in the lung alveolar space after birth, are typically depleted following influenza infection and replaced by bone marrow-derived trans-macrophages [14, 23]. Consistent with this, the number of alveolar macrophages progressively decreased in the infected lungs of both groups, although NOD.SCID mice exhibited a lower number of cells in the early stages of infection compared to CB17.SCID mice (Fig. 1H). Alveolar macrophages are known to play a protective role in influenza infection and have been reported to protect alveolar epithelial cells against IAV infection [24, 25]. Thus, alveolar macrophages may not be the primary contributors to early lethality in CB17.SCID mice.

Higher *Cxcl14* gene expression in the lungs of influenza-infected NOD.SCID mice compared to CB17.SCID mice

To identify a molecular signature associated with attenuated lung inflammation in influenza-infected NOD.SCID mice, we extracted mRNAs from the lungs of

NOD.SCID and CB17.SCID mice one day after IAV challenge. Bulk RNA sequencing analysis was performed, resulting in 1703 differentially expressed genes (DEGs) out of a total of 20,623 genes. The DEGs were filtered based on a p -value < 0.05 and fold change > 2; 827 genes (49%) showed significant downregulation and 876 genes (51%) showed significant upregulation in NOD.SCID mice compared to CB17.SCID mice (Fig. 2A).

To explore the major pathways associated with these DEGs, we conducted pathway analysis using Bioplex 2019 (p -value ranking) in Enrichr (<https://maayanlab.cloud/Enrichr/>). Through this analysis, we identified the top 10 upregulated (Fig. 2B and Additional file 1: Table S1) and downregulated (Fig. 2C and Additional file 1: Table S2) signaling pathways in NOD.SCID mice. Among them, the cytokine-cytokine receptor interaction was confirmed to be the most prominently downregulated pathway in NOD.SCID mice (Fig. 2D, E). In particular, the early response cytokines type I IFN (*ifna4* and *ifnb1*) and type III IFN (*ifnl2* and *ifnl3*) secreted by pulmonary epithelial cells, alveolar macrophages, and plasmacytoid dendritic cells in response to recognition of IAVs were upregulated in CB17.SCID mice [6]. Notably, the upregulation of IFN- λ (*ifnl2* and *ifnl3*), which is restricted to epithelial cells [6], was significantly reduced in NOD.SCID mice, suggesting that the pulmonary epithelial response to IAV infection was reduced in NOD.SCID mice compared to CB17.SCID mice.

Early inflammatory cytokines such as IL-1 (*Il1a*, *Il1b*), IL-6 (*Il6*) and TNF- α (*Tnf*) [6] were markedly reduced in NOD.SCID mice. Similarly, CCL2 (*Ccl2*), a ligand for CCR2 that recruits CCR2⁺ inflammatory monocytes [13], as well as CXCL1 (*Cxcl1*), CXCL2 (*Cxcl2*), and CXCL5 (*Cxcl5*), which are ligands of CXCR2 that induce neutrophil infiltration in influenza-infected lungs [26–28], showed notable decreases in NOD.SCID mice. Likewise, CXCL11 (*Cxcl11*), a ligand of CXCR3 involved in neutrophil recruitment [29], and CCL20, which promotes the migration of immune cells such as monocytes, eosinophils, and NK cells [30], were also significantly lower in NOD.SCID compared to CB17.SCID mice. The downregulated expression of these chemokine genes in the lungs of NOD.SCID mice were further confirmed by quantitative real-time PCR (Fig. 2F). In contrast to many inflammatory cytokines and chemokines, RNA sequencing analysis revealed an upregulation of some cytokine and chemokine genes, particularly the *Cxcl14* gene, in NOD.SCID mice compared to the CB17.SCID control (Fig. 2E). Quantitative real-time PCR analysis confirmed that *Cxcl14* gene expression was significantly higher in NOD.SCID mice than in CB17.SCID mice (Fig. 2G).

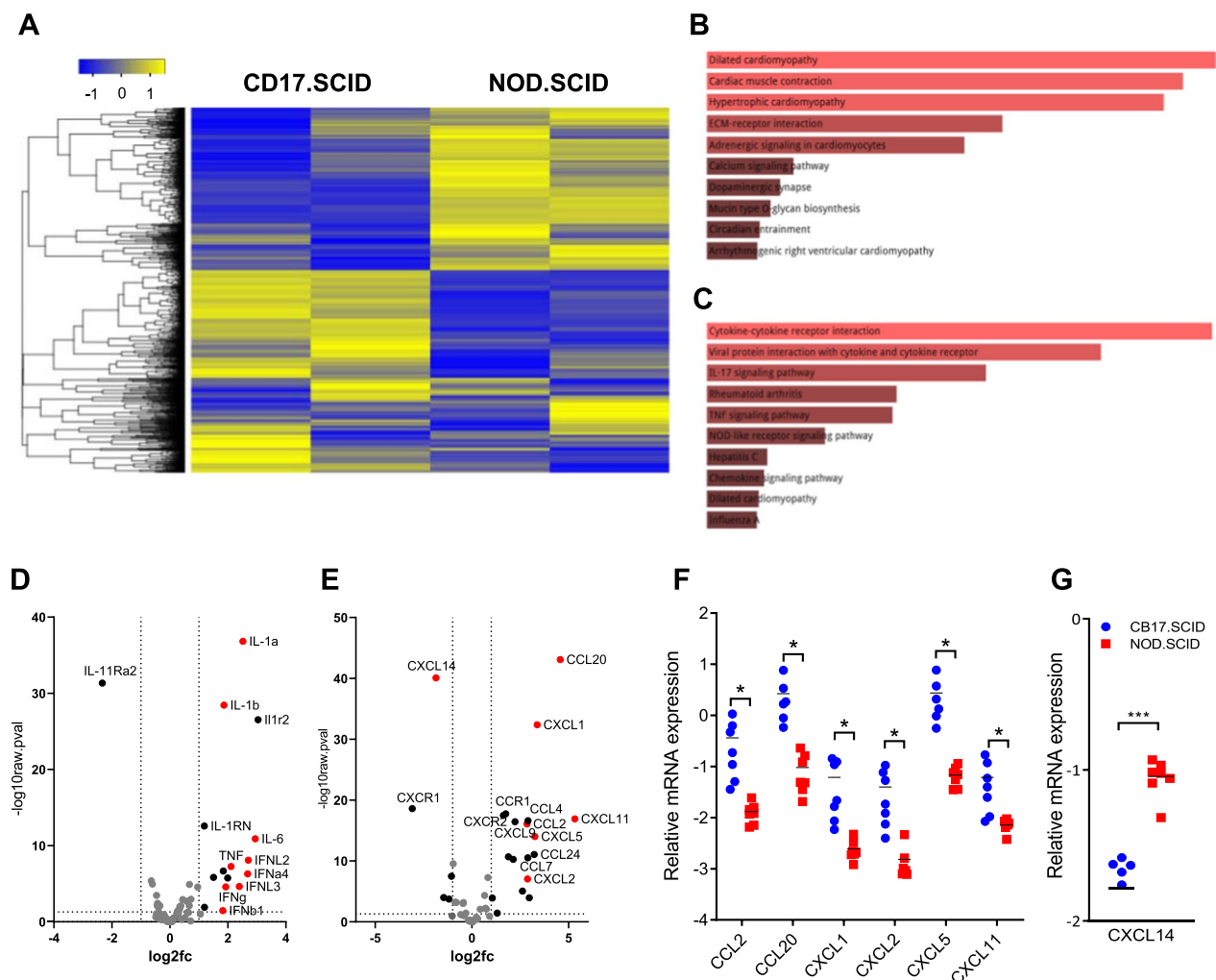


Fig. 2 Comparative analysis of gene expression profiles and selected chemokine genes in IAV-infected lungs of CB17.SCID and NOD.SCID mice. Total mRNA was extracted from the lungs on day 1 post-infection, and bulk RNA sequencing analysis was conducted. **(A)** A heatmap depicting differentially expressed genes between CB17.SCID and NOD.SCID mice ($n = 2$ per group). Gene sets enriched in NOD.SCID **(B)** and CB17.SCID **(C)** mice were analyzed using Bioplanet 2019 with p -value ranking in Enrichr, showing the top 10 dominant pathways within each mouse group. Volcano plots showing differentially expressed cytokine **(D)** and chemokine **(E)** genes between the two groups. The transcript levels of each gene were measured by quantitative reverse transcription real-time PCR, and relative gene expression levels were calculated using *Gapdh* as a control gene. **(F)** Summarized results from two groups of mice ($n = 7$ per group) show statistically significant upregulation of chemokine genes in CB17.SCID lungs compared to those of NOD.SCID mice. **(G)** A summarized graph obtained from the same dataset as **(F)** shows higher expression of *Cxcl14* chemokine genes in NOD.SCID lungs than in CB17.SCID mice on day 1 post-infection. Statistical significance indicated as follows: * $p < 0.05$; *** $p < 0.001$

Protection of mice against lethal influenza infection by inoculation with AAV9-EGFP vector

CXCL14 is a 9.4 kDa chemokine produced by various immune and nonimmune cells, including pulmonary epithelial cells, and involved in diverse functions, such as the modulation of leukocyte migration, differentiation, and antimicrobial activity [31, 32]. Notably, CXCL14 has been reported to inhibit M1 macrophage polarization and pro-inflammatory cytokine production in a sepsis-associated kidney injury model [33]. This raised the possibility that

overexpression of CXCL14 may contribute to the suppression of lung inflammation following influenza infection in NOD.SCID mice.

To investigate this hypothesis, we delivered the *Cxcl14* gene to the lungs of mice using the AAV9-EGFP vector. AAV is known for its nonpathogenicity and low immunogenic nature, enabling long-term expression of therapeutic genes in both animals and humans [15, 16]. Specifically, the AAV9-EGFP vector has recently been utilized to transduce the human ACE2 gene into

mouse airway epithelial cells for the development of a SARS-CoV-2 mouse infection model [34]. Based on this, we delivered the AAV9-EGFP control or AAV9-EGFP-mCXCL14 vectors into the lungs of BALB/c mice through oropharyngeal inoculation, followed by intranasal infection with a lethal dose of IAV. As a negative control, mice were also challenged with IAV without receiving the AAV9-EGFP vector. Increased *Cxcl14* gene expression in AAV9-EGFP-mCXCL14 inoculated lungs was confirmed by qPCR 2 weeks later (Fig. 3A). After IAV infection, the survival time and rate were compared between mice in these three groups. First, mice were infected with IAV two weeks after AAV9 inoculation according to a previously reported protocol [34]. However, no difference in survival time or rate was observed between these three groups (Fig. 3B).

Next, the time interval between vector inoculation and influenza infection was extended to 4 weeks, considering previous reports that indicated progressively increased expression of AAV-transduced genes for more than 12 weeks after intravenous injection of the vectors [35]. Surprisingly, both mice receiving the AAV9-EGFP control or AAV9-EGFP-mCXCL14 vectors exhibited statistically significant survival rates and prolonged survival times compared to naive control mice infected with IAV. Among the mice receiving AAV9-EGFP and AAV9-EGFP-mCXCL14 vectors, 50% (5/10) and 40% (4/10), respectively, were protected from lethal influenza infection, whereas all naive mice experienced 100% mortality (Fig. 3C). Furthermore, morbidity, as indicated by weight loss, was attenuated in both groups of vector-treated mice compared to the naive control (Fig. 3D).

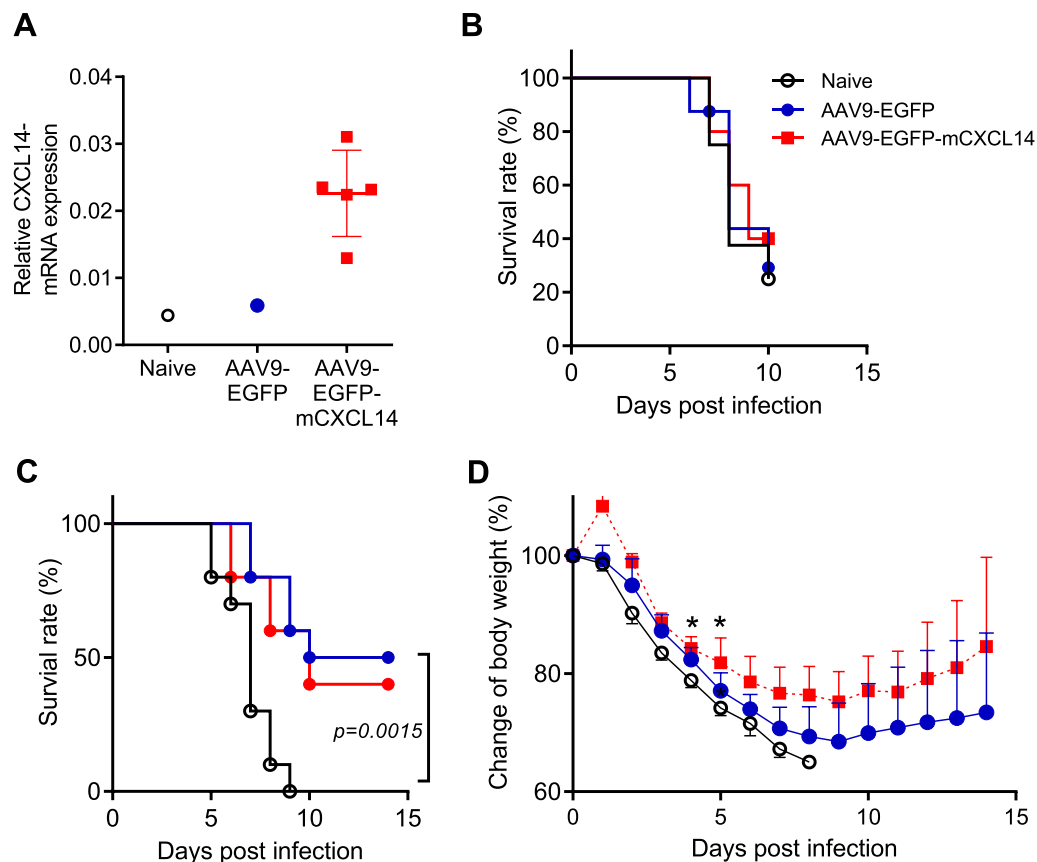


Fig. 3 Protective effect of airway inoculation with the AAV9 vector against lethal influenza infection in mice. **(A)** AAV9-EGFP or AAV9-EGFP-mCXCL14 vectors were administered to BALB/c mice, and lung *Cxcl14* gene expression was quantified by qPCR 2 weeks later. Naive mice were used as negative controls. The AAV9-EGFP-mCXCL14 group exhibited upregulated *mCXCL14* gene expression compared to both the naive and AAV9-EGFP groups. **(B)** Two weeks after AAV9 vector inoculation, mice were infected with IAV. Naive mice infected with IAV served as a control. A summarized survival graph of the three groups ($n=5$ per group) shows no significant difference between the groups. **(C-D)** Mice were infected with IAV 4 weeks after AAV9 vector administration. Cumulative follow-up results from two independent experiments ($n=10$ per group) show reduced mortality **(C)** and attenuated weight loss **(D)** in mice receiving AAV9-EGFP or AAV9-EGFP-mCXCL14 vectors compared to infected naive controls. Statistical analysis was performed using the log-rank (Mantel-Cox) test for survival comparison and multiple t-test for weight change comparison. Statistical significance is indicated as follows: $*p < 0.05$

Subsequently, inflammatory cells in the lungs of AAV9-EGFP vector-treated mice and naive control mice were analyzed by flow cytometry prior to IAV infection (day 0), as well as on days 2 and 4 after infection (Fig. 4A). On day 0, the AAV9 vector-treated group showed higher numbers of monocytes (Ly6C⁻ or Ly6C⁺), NK cells, CD8 T cells, and B cells compared to the naive control group (Additional file 1: Fig. S1). However, by day 4 post-infection, a significant difference in the number of trans-macrophages and neutrophils was observed between the two groups (Fig. 4B, C). Notably, infiltration of trans-macrophages and neutrophils into the infected lungs was attenuated in AAV9 vector-treated mice compared to naive mice. Although the number of NK cells remained higher in the AAV9 vector group on day 2 post-infection, no significant differences were observed in other immune cells, including alveolar macrophages, eosinophils and CD4 T cells (Additional file 1: Fig. S1). Furthermore, the gene expression levels of cytokines, including IFN- β , and chemokines were found to be comparable in the lungs of both groups of mice (Fig. 4D and Additional file 1:

Fig. S2). Finally, to assess whether AAV9 vector inoculation affected IAV replication or clearance, lung viral titers were measured by qPCR, and no significant difference was found between the two groups (Fig. 4E). Taken together, these results suggest that pulmonary AAV9-EGFP vector inoculation may protect mice against lethal influenza infection by inhibiting the migration of neutrophils and trans-macrophages into the infected lung.

Discussion

The main goal of this study was to identify strategies to control influenza-associated lung injury and protect the host against lethal influenza infection. Initially, we focused on comparing the innate immune response between CB17.SCID and NOD.SCID mice. Our findings indicated that NOD.SCID mice, which exhibited attenuated infiltration of neutrophils and inflammatory monocytes, experienced reduced morbidity and mortality compared to CB17.SCID mice. Additionally, an increase in *Cxcl14* chemokine gene expression was observed in infected NOD.SCID lungs. Based on these findings, the

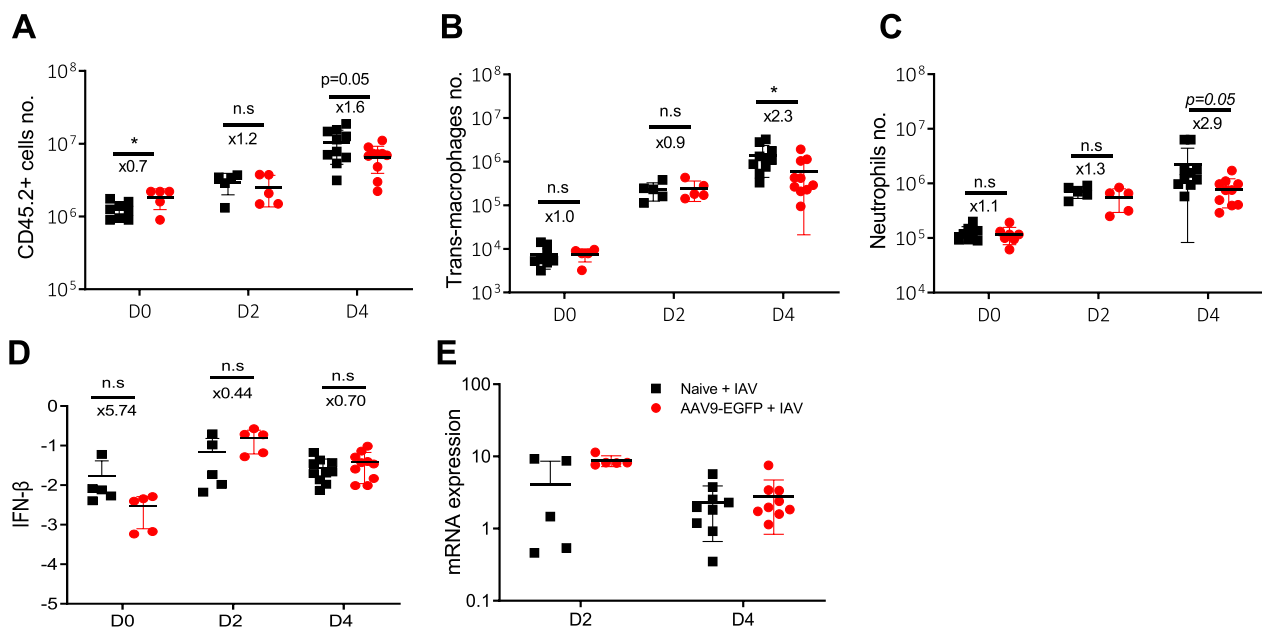


Fig. 4 Comparison of innate cells, cytokines, and virus titers in IAV-infected lungs of naive and AAV9-EGFP vector-treated mice. Cells were isolated from mouse lungs before IAV infection (D0) or on days 2 (D2) and 4 (D4) post-infection, four weeks after AAV9-EGFP vector administration. Absolute numbers of each immune cell were calculated based on flow cytometry analysis: CD45.2⁺ cells (A), trans-macrophages (B), and neutrophils (C). Naive mice infected without pre-administered AAV9 vector were used as controls. Cumulative results from two independent experiments (n = 5–10 per group) show lower numbers of neutrophils and trans-macrophages on day 4 post-infection in the lungs of AAV9 vector-treated mice compared to naive controls. Total mRNA was extracted from mouse lungs before IAV infection (D0) or on days 2 (D2) and 4 (D4) post-infection, four weeks after AAV9-EGFP vector administration. (D) IFN- β gene expression levels were quantified by qPCR and normalized to *Gapdh*. Cumulative results from two independent experiments (n = 5–10 per group) showed no significant difference between the two groups. (E) Total mRNAs were extracted from the lungs of mice infected with IAV in the presence or absence of pre-administered AAV9 vector. Levels of IAV N gene transcripts were measured by quantitative PCR, with *Gapdh* as a control gene for relative expression. Cumulative results from two independent experiments (n = 5–10 per group) show no difference in IAV gene expression levels in between the two groups. The data are means \pm SDs; the x-values are fold changes. Statistical significance is indicated as follows: * $p < 0.05$

Cxcl14 gene was delivered to the lungs of mice using the AAV9-EGFP vector to investigate whether *Cxcl14* over-expression could alleviate inflammatory cell infiltration in IAV-infected lungs. Contrary to expectations, mice receiving the AAV9 vector with the *Cxcl14* gene prior to IAV infection showed similar morbidity in terms of weight loss and mortality compared to mice receiving a control AAV9 vector. However, approximately half of the hosts in both groups survived, whereas all naive mice that did not receive the AAV9 vector succumbed early after IAV challenge. Further analysis revealed that AAV9 vector inoculation into the respiratory tract resulted in reduced infiltration of neutrophils and trans-macrophages in the infected lungs.

When BALB/c, CB17.SCID, and NOD.SCID mice were infected with IAV, and only BALB/c mice were able to recover after initial weight loss, while both CB17.SCID and NOD.SCID, lacking adaptive immune cells, failed to survive due to inadequate virus control, as expected. Furthermore, there was no significant difference in weight loss between BALB/c and CB17.SCID mice during the first 5 days, when adaptive immunity might not be fully activated to participate in virus control [6]. However, NOD.SCID mice exhibited a slower decline in body weight and longer survival compared to CB17.SCID mice, despite similar virus titers in all three groups. Flow cytometric analysis revealed that exaggerated infiltration of neutrophils and inflammatory monocytes was associated with severe morbidity and shortened survival in CB17.SCID mice. These findings support previous reports suggesting that attenuation of neutrophil and monocyte infiltration in influenza-infected lungs has beneficial effects on host morbidity and mortality [11, 13, 14].

One of the notable findings from the initial experiments in this study was that an inverse relationship was identified between the expression level of the *Cxcl14* gene and the degree of inflammatory cell influx in infected lungs. CXCL14 has been previously suggested to have an anti-inflammatory effect [33, 36]. However, TNF- α can downregulate *Cxcl14* expression [37], and the absence of CXCL14 does not affect the severity of IAV infection [38]. In our current study, we observed much higher levels of TNF- α in severely inflamed CB17.SCID lungs in contrast to NOD.SCID lungs. We also found that the delivery of the *Cxcl14* gene using AAV9 vectors into the mouse airway failed to demonstrate beneficial effects of CXCL14 chemokine on the survival of IAV-infected hosts. These results suggest that the elevated expression of *Cxcl14* in the infected lungs of NOD.SCID mice might be a consequence of reduced TNF- α levels, rather than indicative of the anti-inflammatory effect of this chemokine.

In this study, the administration of AAV9 vectors containing only EGFP, which are commonly used as control vectors in gene transfer experiments with AAV9 vectors, showed a prophylactic effect against lethal influenza infection. Interestingly, this effect was observed only when the AAV9 vector was inoculated 4 weeks prior to IAV infection, not 2 weeks. A previous report demonstrated that intranasal instillation of replication-deficient adenovirus (E1 & E3 gene-deleted Ad5 empty, AdE) particles without a transgene also protected BALB/c mice against lethal IAV infection [39]. However, AdE particles were administered 2 days prior to IAV challenge, and their effect was attributed to the rapid induction of inflammatory cytokines/chemokines and the antiviral response, although the specific mechanisms were not well understood. In contrast to adenovirus particles, AAV vectors are known not to induce acute inflammation [16]. Moreover, the main feature observed in AAV9-treated mice in the current study was the attenuated infiltration of neutrophils and trans-macrophages in IAV-infected lungs, suggesting that the prophylactic mechanisms of AAV9 and AdE may be different.

Although AAV vectors are generally considered to have low immunogenicity, their immunogenicity can be dose dependent, and adaptive immune responses against the transgene product and viral cap protein can limit their long-term efficacy [16, 40]. Moreover, the double-stranded DNA (dsDNA) vector genome can trigger innate immunity [40]. Notably, a previous study demonstrated that dsRNA transcribed from viral dsDNA can promote IFN- β production in host cells [20]. This IFN- β can suppress AAV transgene expression *in vivo* and *in vitro*, and the production of IFN- β in host cells is dependent on the MDA5 dsRNA sensor, suggesting that dsRNA can trigger IFN- β production. This possibility was further confirmed by the detection of transgene-derived minus strand transcripts, which are essential for dsRNA formation. Interestingly, the level of IFN- β induction in humanized mice was higher at 8 weeks compared to 4 weeks after injection of the AAV vector carrying the human Factor IX gene [20]. On the other hand, other research has shown that transgene expression levels progressively increased after gene delivery using AAV vectors, especially for more than 12 weeks in mice [35], suggesting that the levels of IFN- β induction correlate with transgene expression levels. These previous findings can explain why the prophylactic effect of the AAV9 vector was observed at 4 weeks rather than 2 weeks after vector administration, as observed in the current study.

This study has certain limitations in terms of fully understanding the prophylactic mechanism of the AAV9 vector. The specific mechanisms involved were not thoroughly documented in the current study. While the

increased infiltration of monocytes, NK cells and CD8 T cells in the lungs of AAV9-inoculated mice may contribute to early viral control, no significant difference in viral gene expression levels was observed between the AAV9 and control groups. Alternative explanations could include IFN- β production triggered by dsRNA generated from the transgene, which may induce antiviral genes in the alveolar epithelium, the primary host cell of the AAV9 vector. Another possibility is that long-term exposure to low levels of IFN- β may lead to desensitization of innate immune cells. However, no significant increase in IFN- β gene expression was observed in AAV9 vector-treated mice compared to naive control mice. To re-evaluate this finding, it is crucial to assess the expression of the IFN- β gene specifically in isolated lung epithelial cells and investigate the potential elimination of the protective effect of the AAV9 vector by blocking IFN- β activity. Additionally, conducting studies that deplete neutrophils or monocytes could clarify whether the presence of these cells is necessary for the protective effect of the AAV vector.

Conclusions

This study demonstrates a potential strategy for controlling lung immunopathology following severe influenza infection. To control lung inflammation, BALB/c mice were infected with IAV following AAV9 inoculation, which resulted in attenuated infiltration of trans-macrophages, neutrophils and monocytes in the lungs. These findings imply that pre-inoculation with AAV9 prior to IAV infection protected mouse lungs from immunopathology by reducing the recruitment of inflammatory cells. Although there was no difference in lung viral titers between the naive group and the AAV9 pre-inoculated group, this study represents the first report demonstrating the protective effect of the AAV vector in a severe influenza infection model.

Methods

Animals

BALB/c, NOD.SCID and CB17.SCID mice were obtained from Central Lab. Animal Inc. (Seoul, South Korea). These mice were housed in sterilized cages with access to sterilized food and water at the laboratory animal facility of the Biomedical Center for Animal Resource Development at Seoul National University, as well as the Biomedical Research Institute of Seoul National University Hospital (Seoul, South Korea). The mice used in this study were 6 weeks old with an average body weight of 18 g. Ethical approval for this study was obtained from the Institutional Animal Care and Use Committee (IACUC) of the Seoul National University Institute of Laboratory Animal Resource (IACUC Number:

220221-3-2) and the Biomedical Research Institute of Seoul National University Hospital (IACUC number: 22-0235-S1A1). All experimental procedures were conducted in compliance with international and institutional guidelines.

Experimental group and monitoring

To assess the severity of IAV infection, BALB/c, CB17.SCID, and NOD.SCID mice were intranasally infected with IAV. CB17.SCID mice and NOD.SCID mice were infected with IAV and sacrificed on days 1, 3, and 5 for flow cytometry analysis. CB17.SCID and NOD.SCID mice were used for bulk RNA sequencing analysis 1 day after IAV infection. Daily weight measurements were recorded for all mice after IAV infection. For the AAV9 vector experiment, BALB/c mice were divided into three groups as follows: the naive group received no treatment, group 2 was inoculated with AAV9-EGFP only, and group 3 was inoculated with AAV9-EGFP-mCXCL14 containing the murine *Cxcl14* gene. Subsequently, these mice were infected with IAV 2 weeks later. Second, BALB/c mice were divided into two groups as follows: the naive group received no treatment, and group 2 was inoculated with AAV9-EGFP only. Subsequently, these mice were infected with IAV 4 weeks later. Daily weight measurements were recorded for all mice after IAV infection. All mice were sacrificed 0, 2, and 4 days after IAV infection to analyze inflammatory cell infiltration and gene expression in the infected lungs.

Virus preparation, AAV production, infection, and tissue harvest

The influenza virus strain A/PR/8/34 (PR8, H1N1) was used in this study. Viral stocks were obtained by transfecting MDCK cells, as provided by Pr. YK Choi's laboratory (Chungbuk National University, Chungbuk, South Korea). The virus was harvested 24 h after transfection and stored at -80°C until use. For infection, mice were anesthetized with isoflurane and oxygen. Intranasal infection was performed by administering 50 μl of phosphate buffered saline (PBS) containing IAV at a dose of 3.5×10^5 PFU/ml, ensuring deposition of the virus in the lower respiratory tract. AAV9-EGFP and AAV9-EGFP-mCXCL14 vectors were purchased from Vector Builder (Chicago, Illinois, USA) as 2×10^{13} stocks and administered to mice via oropharyngeal delivery under anesthesia. A bolus inoculation of 50 μl of AAV9-EGFP at a dose of 10^{11} GC (genome copies) per mouse was given using a pipette. Infection procedures were performed in a biosafety level 2 laboratory in accordance with the animal facility guidelines of the Biomedical Research Institute of Seoul National University Hospital. Lung tissues were harvested with PBS and cut using a razor. Dissociation

medium was prepared by adding 50 μ l of collagenase type IV (0.1 g/ml, Worthington Biochemical Corporation, NJ, USA) and 50 μ l of DNase I solution (1 mg/ml, Sigma, St. Louis, Missouri, USA) to 50 ml of RPMI 1640 medium and incubated at 37 °C for 2 h on a shaking platform.

Preprocessing and analysis of bulk RNA-Seq data and gene enrichment

The infected lungs from euthanized mice were homogenized with DMEM, and lung tissue was used for RNA isolation using a BIO-52072 RNA isolation kit from Meridian Bioscience (Memphis, TN, USA). Next-generation sequencing (NGS) was performed using the Illumina NovaSeq platform at Macrogen (Seoul, South Korea). The clean reads obtained were mapped to the genome, and transcripts were assembled and merged using StringTie v2.1.3b with corresponding genome annotation. Genes with a *p* value less than 0.05 and a fold change greater than 2 were selected for gene set enrichment analysis in Enrichr (<https://maayanlab.cloud/Enrichr/>).

Flow cytometry analysis

Mononuclear cells were isolated from the lungs of infected or uninfected mice. The samples were stained with specific monoclonal antibodies including Ly6G (1A8), CD11b (M1/70), CD11c (N418), CD49b (DX5), F4/80 (BM8), CD45.2 (104), CD64 (X54-5/7.1), Siglec F (E50-2440), and Ly6C (HK1.4). These antibodies were obtained from BD Bioscience (San Jose, CA, USA), eBioscience (San Diego, CA, USA), and BioLegend (San Diego, CA, USA). The prepared cells were resuspended in staining buffer (PBS, 0.5% bovine serum albumin, and 0.5 mM EDTA), and single-cell suspensions were labeled with antibodies for 30 min at 4 °C. Flow cytometry analysis was performed using an LSRFortessa X-20 instrument from BD Bioscience, and the acquired data were analyzed using FlowJo software v10 from TreeStar (San Carlos, USA).

Quantitative real-time PCR

Lung tissue was processed to extract total RNA using the Total RNA Isolation Kit (BIO-52072, Meridian Bioscience) following the manufacturer's instructions. cDNA synthesis was performed using AccuPower Cycle Script RT PreMix (Bioneer) with the extracted RNA. The expression levels of the IAV gene (NS), CCL2, CCL20, CXCL1, CXCL2, CXCL5, CXCL11, CXCL14, and glyceraldehyde-3-phosphate dehydrogenase (GAPDH) were assessed by qPCR analysis. The sequences of primers used for qPCR can be found in Additional file 1: Table S3. The qPCR included 1 μ l of cDNA (0.5 μ g/ μ l), 1 μ l of each primer, and 5 μ l of PowerUp SYBR Green Master Mix (A25742, Applied Biosystems, Framingham, MA, USA).

qPCR was performed using a CFX Connect real-time PCR instrument (Applied Biosystems). The PCR program consisted of an initial incubation at 95 °C for 10 min, followed by 40 cycles of 15 s at 95 °C and 60 s at 60 °C, and a final step of 95 °C for 15 s, 60 °C for 60 s, and 95 °C for 15 s. The gene expression levels were quantified using SYBR-Green, and the relative expression of RNA was normalized to the internal control GAPDH.

Statistical analysis

Statistical analysis was conducted using GraphPad Prism version 8.0 (GraphPad Software Inc., San Diego, CA, USA). The data are presented as the mean of experimental measurements with standard deviation (SD). Statistical significance was determined using the t-test, and *p* values less than 0.05 were considered statistically significant.

Abbreviations

AAV	Adeno-associated virus
Cap	Capsid
cDNA	Complementary DNA
DEG	Differentially expressed genes
dsRNA	Double stranded RNA
EGFP	Enhanced green fluorescent protein
GC	Genomic copies
HA	Hemagglutinin
IAV	Influenza A virus
IFN	Interferon
ITR	Inverted terminal repeats
mCXCL14	Murine-CXCL14
NA	Neuraminidase
PBS	Phosphate buffered saline
qPCR	Reverse transcription quantitative real-time PCR
Rep	Replication
TCR	T-cell receptor

Supplementary Information

The online version contains supplementary material available at <https://doi.org/10.1186/s42826-023-00177-0>.

Additional file 1: Table S1. Top 10 upregulated signaling pathways in NOD.SCID mice vs. CD17.SCID mice lungs. **Table S2.** Top 10 downregulated signaling pathways in NOD.SCID mice vs. CD17.SCID mice lungs. **Table S3.** Sequences of primers (mouse) used for qPCR. **Fig. S1.** Comparison of immune cells in IAV-infected lungs of AAV9-EGFP vector-treated and naive control mice. **Fig. S2.** Comparison of cytokine and chemokine gene expression in IAV-infected lungs of AAV9-EGFP vector-treated and naive control mice.

Acknowledgements

We thank Professor Young Ki Choi of Chungbuk National University for providing us with the influenza A virus.

Author contributions

E.A.C. designed and performed the experiments, sample preparation, and animal experiments and analyzed the data. H.J.P. and S.M.C. provided technical assistance and optimized the protocols. J.I.L. contributed to the experimental design, data analysis and manuscript preparation. K.C.J. was a major

contributor to the experimental design, funding management and writing the manuscript. All authors have read and approved the final manuscript.

Funding

This study was supported by grants from the National Research Foundation funded by the Korean government (Grant No. 2022R1F1A1063764) and the Research Fund from Seoul National University Hospital (Grant No. 0420210230).

Availability of data and materials

The datasets used and/or analyzed during the current study are available from the corresponding author on reasonable request.

Declarations

Competing interests

All authors have disclosed that there are no conflicts of interest in this work.

Author details

¹Graduate Course of Translational Medicine, Seoul National University College of Medicine, Seoul 03080, Republic of Korea. ²Transplantation Research Institute, Seoul National University College of Medicine, Seoul 03080, Republic of Korea. ³Department of Pathology, Seoul National University College of Medicine, Seoul 03080, Republic of Korea. ⁴Integrated Major in Innovative Medical Science, Seoul National University Graduate School, Seoul 03080, Republic of Korea. ⁵Department of Medicine, Seoul National University College of Medicine, Seoul 03080, Republic of Korea.

Received: 28 August 2023 Revised: 10 October 2023 Accepted: 20 October 2023

Published online: 30 October 2023

References

- Dawson WK, Lazniewski M, Plewczynski D. RNA structure interactions and ribonucleoprotein processes of the influenza A virus. *Brief Funct Genom.* 2018;17(6):402–14.
- Shao W, Li X, Goraya MU, Wang S, Chen JL. Evolution of influenza A virus by mutation and re-assortment. *Int J Mol Sci.* 2017;18(8):1650.
- Smith GJ, Bahl J, Vijaykrishna D, Zhang J, Poon LL, Chen H, et al. Dating the emergence of pandemic influenza viruses. *Proc Natl Acad Sci U S A.* 2009;106(28):11709–12.
- Gu Y, Zuo X, Zhang S, Ouyang Z, Jiang S, Wang F, et al. The mechanism behind influenza virus cytokine storm. *Viruses.* 2021;13(7):1362.
- Perrone LA, Plowden JK, Garcia-Sastre A, Katz JM, Tumpey TM. H5N1 and 1918 pandemic influenza virus infection results in early and excessive infiltration of macrophages and neutrophils in the lungs of mice. *PLoS Pathog.* 2008;4(8):e1000115.
- Latino I, Gonzalez SF. Spatio-temporal profile of innate inflammatory cells and mediators during influenza virus infection. *Curr Opin Physiol.* 2021;19:175–86.
- George ST, Lai J, Ma J, Stacey HD, Miller MS, Mullarkey CE. Neutrophils and influenza: a thin line between helpful and harmful. *Vaccines (Basel).* 2021;9(6):597.
- Peiro T, Patel DF, Akthar S, Gregory LG, Pyle CJ, Harker JA, et al. Neutrophils drive alveolar macrophage IL-1 β release during respiratory viral infection. *Thorax.* 2018;73(6):546–56.
- Tate MD, Brooks AG, Reading PC, Mintern JD. Neutrophils sustain effective CD8(+) T-cell responses in the respiratory tract following influenza infection. *Immunol Cell Biol.* 2012;90(2):197–205.
- Lim K, Hyun YM, Lambert-Emo K, Capece T, Bae S, Miller R, et al. Neutrophil trails guide influenza-specific CD8(+) T cells in the airways. *Science.* 2015;349(6252):aaa4352.
- Brandes M, Klauschen F, Kuchen S, Germain RN. A systems analysis identifies a feedforward inflammatory circuit leading to lethal influenza infection. *Cell.* 2013;154(1):197–212.
- Palomino-Segura M, Perez L, Farsakoglu Y, Virgilio T, Latino I, D'Antuono R, et al. Protection against influenza infection requires early recognition by inflammatory dendritic cells through C-type lectin receptor SIGN-R1. *Nat Microbiol.* 2019;4(11):1930–40.
- Lin SJ, Lo M, Kuo RL, Shih SR, Ojcius DM, Lu J, et al. The pathological effects of CCR2+ inflammatory monocytes are amplified by an IFNAR1-triggered chemokine feedback loop in highly pathogenic influenza infection. *J Biomed Sci.* 2014;21(1):99.
- Coates BM, Staricha KL, Koch CM, Cheng Y, Shumaker DK, Budinger GRS, et al. Inflammatory monocytes drive Influenza A virus-mediated lung injury in Juvenile mice. *J Immunol.* 2018;200(7):2391–404.
- Kessler PD, Podsakoff GM, Chen X, McQuiston SA, Colosi PC, Matelis LA, et al. Gene delivery to skeletal muscle results in sustained expression and systemic delivery of a therapeutic protein. *Proc Natl Acad Sci U S A.* 1996;93(24):14082–7.
- Zaiss AK, Muruve DA. Immune responses to adeno-associated virus vectors. *Curr Gene Ther.* 2005;5(3):323–31.
- Li C, Samulski RJ. Engineering adeno-associated virus vectors for gene therapy. *Nat Rev Genet.* 2020;21(4):255–72.
- McCarty DM. Self-complementary AAV vectors; advances and applications. *Mol Ther.* 2008;16(10):1648–56.
- Au HKE, Isalan M, Mielcarek M. Gene therapy advances: a meta-analysis of AAV usage in clinical settings. *Front Med (Lausanne).* 2021;8:809118.
- Shao W, Earley LF, Chai Z, Chen X, Sun J, He T, et al. Double-stranded RNA innate immune response activation from long-term adeno-associated virus vector transduction. *JCI Insight.* 2018;3(12):e120474.
- Channappanavar R, Fehr AR, Vijay R, Mack M, Zhao J, Meyerholz DK, et al. Dysregulated type I interferon and inflammatory monocyte-macrophage responses cause lethal pneumonia in SARS-CoV-infected mice. *Cell Host Microbe.* 2016;19(2):181–93.
- Lin KL, Sweeney S, Kang BD, Ramsburg E, Gunn MD. CCR2-antagonist prophylaxis reduces pulmonary immune pathology and markedly improves survival during influenza infection. *J Immunol.* 2011;186(1):508–15.
- Li F, Piattini F, Pohlmeier L, Feng Q, Rehrauer H, Kopf M. Monocyte-derived alveolar macrophages autonomously determine severe outcome of respiratory viral infection. *Sci Immunol.* 2022;7(73):eabj5761.
- Somerville L, Cardani A, Braciale TJ. Alveolar macrophages in Influenza A infection guarding the castle with sleeping dragons. *Infect Dis Ther (San Antonio).* 2020. <https://doi.org/10.31038/iddt.2020114>.
- Cardani A, Boulton A, Kim TS, Braciale TJ. Alveolar macrophages prevent lethal influenza pneumonia by inhibiting infection of type-1 alveolar epithelial cells. *PLoS Pathog.* 2017;13(1):e1006140.
- Ferrero MR, Garcia CC, Dutra de Almeida M, Braz T, da Silva J, Bianchi Reis Insuela D, Teixeira Ferreira TP, et al. CCR5 antagonist maraviroc inhibits acute exacerbation of lung inflammation triggered by influenza virus in cigarette smoke-exposed mice. *Pharmaceuticals (Basel).* 2021;14(7):620.
- Tavares LP, Garcia CC, Machado MG, Queiroz-Junior CM, Barthelemy A, Trottein F, et al. CXCR1/2 antagonism is protective during influenza and post-influenza pneumococcal infection. *Front Immunol.* 2017;8:1799.
- Duemmler A, Montes-Vizuet AR, Cruz JS, Teran LM. CXCL5 into the upper airways of children with influenza A virus infection. *Rev Med Inst Mex Seguro Soc.* 2010;48(4):393–8.
- Rudd JM, Pulavendran S, Ashar HK, Ritchey JW, Snider TA, Malayer JR, et al. Neutrophils induce a novel chemokine receptors repertoire during influenza pneumonia. *Front Cell Infect Microbiol.* 2019;9:108.
- Luo C, Liu J, Qi W, Ren X, Lu R, Liao M, et al. Dynamic analysis of expression of chemokine and cytokine gene responses to H5N1 and H9N2 avian influenza viruses in DF-1 cells. *Microbiol Immunol.* 2018;62(5):327–40.
- Lu J, Chatterjee M, Schmid H, Beck S, Gawaz M. CXCL14 as an emerging immune and inflammatory modulator. *J Inflamm (Lond).* 2016;13:1.
- Shaykhiyev R, Sackrowitz R, Fukui T, Zuo WL, Chao IW, Strulovici-Barel Y, et al. Smoking-induced CXCL14 expression in the human airway epithelium links chronic obstructive pulmonary disease to lung cancer. *Am J Respir Cell Mol Biol.* 2013;49(3):418–25.
- Lv J, Wu ZL, Gan Z, Gui P, Yao SL. CXCL14 overexpression attenuates sepsis-associated acute kidney injury by inhibiting proinflammatory cytokine production. *Mediators Inflamm.* 2020;2020:2431705.
- Israelow B, Song E, Mao T, Lu P, Meir A, Liu F, et al. Mouse model of SARS-CoV-2 reveals inflammatory role of type I interferon signaling. *J Exp Med.* 2020;217(12):e20201241.

35. Palomeque J, Chemaly ER, Colosi P, Wellman JA, Zhou S, Del Monte F, et al. Efficiency of eight different AAV serotypes in transducing rat myocardium in vivo. *Gene Ther.* 2007;14(13):989–97.
36. Rajasekaran G, Dinesh Kumar S, Nam J, Jeon D, Kim Y, Lee CW, et al. Antimicrobial and anti-inflammatory activities of chemokine CXCL14-derived antimicrobial peptide and its analogs. *Biochim Biophys Acta Biomembr.* 2019;1861(1):256–67.
37. Maerki C, Meuter S, Liebi M, Muhlemann K, Frederick MJ, Yawalkar N, et al. Potent and broad-spectrum antimicrobial activity of CXCL14 suggests an immediate role in skin infections. *J Immunol.* 2009;182(1):507–14.
38. Sidahmed AM, Leon AJ, Banner D, Kelvin AA, Rowe T, Boudakov I, et al. CXCL14 deficiency does not impact the outcome of influenza or *Escherichia coli* infections in mice. *J Infect Dev Ctries.* 2014;8(10):1301–6.
39. Zhang J, Tarbet EB, Feng T, Shi Z, Van Kampen KR, Tang DC. Adenovirus-vectored drug-vaccine duo as a rapid-response tool for conferring seamless protection against influenza. *PLoS ONE.* 2011;6(7):e22605.
40. Verdera HC, Kuranda K, Mingozzi F. AAV vector immunogenicity in humans: a long journey to successful gene transfer. *Mol Ther.* 2020;28(3):723–46.

Publisher's Note

Springer Nature remains neutral with regard to jurisdictional claims in published maps and institutional affiliations.

Ready to submit your research? Choose BMC and benefit from:

- fast, convenient online submission
- thorough peer review by experienced researchers in your field
- rapid publication on acceptance
- support for research data, including large and complex data types
- gold Open Access which fosters wider collaboration and increased citations
- maximum visibility for your research: over 100M website views per year

At BMC, research is always in progress.

Learn more biomedcentral.com/submissions

